ACS central science

http://pubs.acs.org/journal/acscii

Research Article

Conversion of Reactive Carbon Solutions into CO at Low Voltage and High Carbon Efficiency

Zishuai Zhang,[⊥] Eric W. Lees,[⊥] Shaoxuan Ren, Benjamin A. W. Mowbray, Aoxue Huang, and Curtis P. Berlinguette*

Cite This: *ACS Cent. Sci.* 2022, 8, 749–755

Read Online

ACCESS | Metrics & More | Article Recommendations | Supporting Information

ABSTRACT: Electrolyzers are now capable of reducing carbon dioxide (CO_2) into products at high reaction rates but are often characterized by low energy efficiencies and low CO_2 utilization efficiencies. We report here an electrolyzer that reduces 3.0 M $KHCO_3$(aq) into CO(g) at a high rate (partial current density for CO of 220 mA cm^{-2}) and a CO_2 utilization efficiency of 40%, at a voltage of merely 2.3 V. These results were made possible by using: (i) a reactive carbon solution enriched in $KHCO_3$ as the feedstock instead of gaseous CO_2; (ii) a cation exchange membrane instead of an anion exchange membrane, which is common to the field; and (iii) the hydrogen oxidation reaction (HOR) at the anode instead of the oxygen evolution reaction (OER). The voltage reported here is the lowest reported for any CO_2 to CO electrolyzer that operates at high current densities (i.e., a partial current density for CO greater than 200 mA cm^{-2}) with a CO_2 utilization efficiency of greater than 20%. This study highlights how the choice of feedstock, membrane, and anode chemistries affects the rate and efficiency at which CO_2 is converted into products.

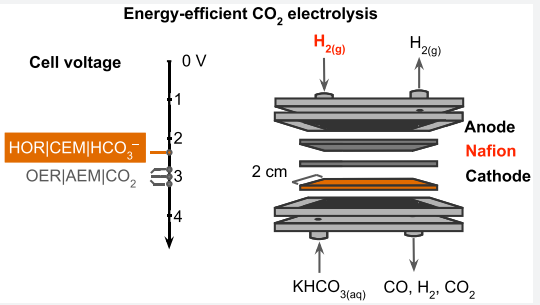

The CO_2 reduction reaction (CO2RR) is a means of using electricity to convert CO_2 into fuels and chemicals.[1−4] A commercial CO2RR electrolyzer will likely need to operate at current densities (j) greater than 200 mA cm^{-2} and cell voltages (V_{cell}) below 3 V.[5−9] The only laboratory-scale CO2RR electrolyzers that meet these criteria use anion exchange membranes (AEMs) to separate the cathode and anode compartments.[9−12] The AEM creates an alkaline environment at the cathode and anode electrodes.[13] The alkalinity at the anode reduces the applied potential required to drive the oxygen evolution reaction (OER) and enables the use of inexpensive nickel electrodes.[14] However, the alkalinity at the cathode also converts the CO_2 reactant into (bi)carbonates (eq 1).[15,16] This situation is problematic because (bi)-carbonates are electrochemically inert and can migrate across the AEM to react with H^+ in the anode chamber to regenerate CO_2.[9,14] Consequently, the maximum possible CO_2 utilization efficiency (eq 2) for CO production is 50% for a CO2RR electrolyzer that does not neutralize the OH^- byproduct (Figure 1); that is, one molecule of CO is produced for every two molecules of CO_2 entering the electrolyzer at steady state.[17] In practice, CO_2 utilization efficiencies of <20% are generally observed for CO2RR electrolyzers that contain an AEM to separate the OER and CO2RR in the anode and cathode chambers, respectively (denoted "**OER|AEM|CO_2**" to indicate the anode|membrane|cathode configuration).[18] Moreover, the O_2 produced at the anode of **OER|AEM|CO_2** electrolyzers has little economic value and is therefore not utilized.[14]

$$CO_2(aq) + 2OH^-(aq) \rightleftharpoons CO_3^{2-}(aq) + H_2O(l) \quad (1)$$

$$CO_2 \text{ utilization efficiency} = \frac{\text{moles of CO produced}}{\text{moles of CO produced} + \text{moles of unreacted } CO_2} \times 100\% \quad (2)$$

CO2RR electrolyzers that use bipolar membranes (BPMs) instead of AEMs convert a larger fraction of the CO_2 feedstock into CO (Figure 1).[20−22] BPMs dissociate water at the interface of an AEM and a CEM to deliver OH^- and H^+ to the anode and cathode, respectively (eq 3). The H^+ supplied to the cathode reacts with bicarbonate to form CO_2 *in situ* (eq 4). The H^+ also neutralizes the OH^- product formed during CO2RR electrolysis (eq 5), which negates the alkalinity problem encountered with AEMs.[23] However, at high current densities a significant potential is required to dissociate water into H^+ and OH^- using a BPM.[24] This potential can be reduced using a water dissociation catalyst.[25] However, CO2RR electrolyzers that use BPMs currently require much

Received: March 22, 2022
Published: May 31, 2022

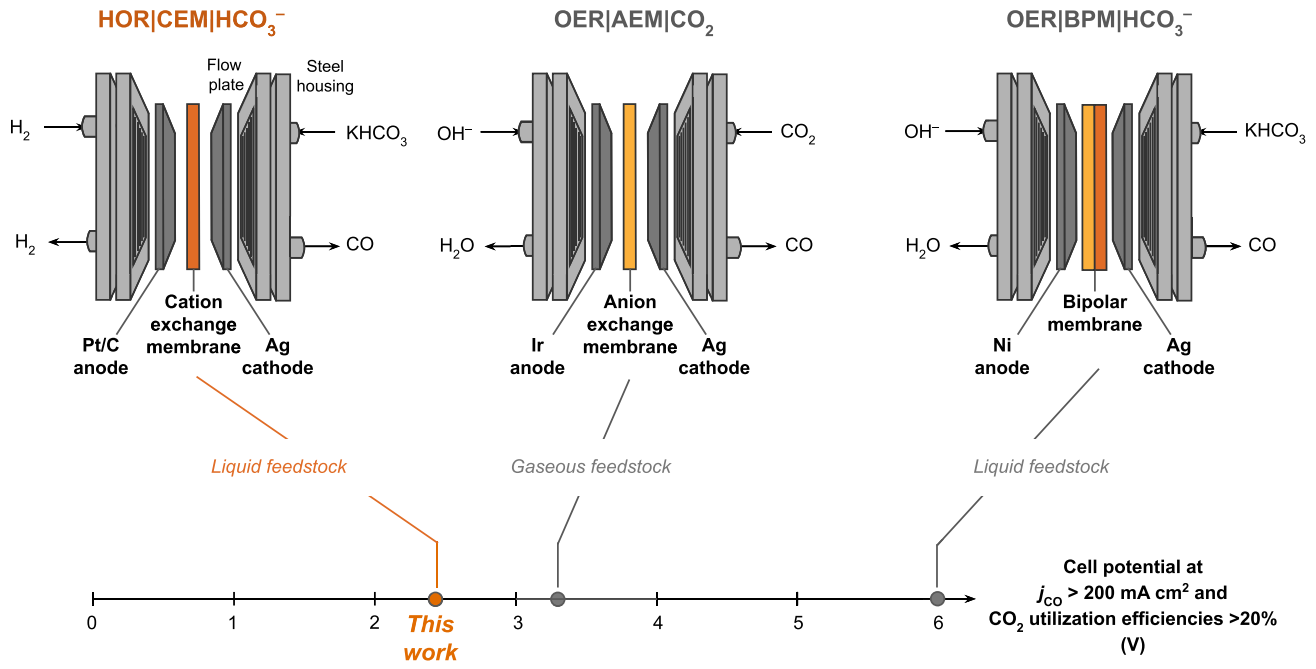

Figure 1. Schematics and nomenclature of prototypical CO_2 to CO electrolyzer configurations. The electrolyzer reported in this work is **HOR|CEM|HCO_3^-**, which uses a reactive carbon solution feedstock, a cation exchange membrane (CEM), and hydrogen oxidation at the anode to achieve low voltages and high CO_2 utilization efficiencies. The **OER|AEM|CO_2** electrolyzer is a widely used architecture that uses a gaseous CO_2 feedstock. The **OER|BPM|HCO_3^-** electrolyzer also uses a reactive carbon solution feedstock, but the BPM needs to be optimized to achieve lower applied cell voltages. The lowest cell voltages reported in the literature for each electrolyzer architecture are indicated, but only the electrolyzers that produce j_{CO} >200 mA cm^{-2} and CO_2 utilization efficiency >20% are considered.[9,19] The nomenclature follows "anode|membrane|cathode".

more than 3 V to realize j_{CO} >200 mA cm^{-2} (Figure 1).[14] It is for these reasons that neither a BPM or an AEM electrolyzer has simultaneously demonstrated high CO_2 utilizations and low voltages (Figure 1).[20,26−29]

$$H_2O(l) \rightarrow H^+(aq) + OH^-(aq) \quad (3)$$

$$H^+(aq) + HCO_3^-(aq) \rightarrow CO_2(aq) + H_2O(l) \quad (4)$$

$$CO_2(aq) + H_2O(l) + 2e^- \rightarrow CO(g) + 2OH^-(aq) \quad (5)$$

Another factor to consider is where the gaseous CO_2 feedstock is derived from. This feedstock requires the isolation, purification, and compression of CO_2 before it enters a CO2RR electrolyzer.[30,31] The isolation of CO_2 from air capture streams requires 23 MJ to convert 100 mol of K_2CO_3 into CO_2,[30] and CO_2 compression requires 2 MJ per 100 mol of CO_2.[32] These steps are capital intensive, and the energy penalties are significant relative to electrolysis (12 MJ per 100 mol CO_2; Table S1). Moreover, the low CO_2 utilization efficiencies obtained with **OER|AEM|CO_2** electrolyzers increase the cost of separating unreacted CO_2 from the product stream.[33]

We report here a "bicarbonate electrolyzer" that solves the aforementioned problems by (i) reducing "reactive carbon solutions" (instead of gaseous CO_2) into CO at the cathode, (ii) replacing the AEM with a CEM, and (iii) replacing the OER with the HOR at the anode. Reactive carbon solutions are defined herein as the aqueous eluent from carbon capture units that use hydroxide to capture CO_2. These bicarbonate-enriched solutions enable captured carbon to be delivered to the electrolyzer as a liquid (e.g., $KHCO_3$(aq)) rather than as gaseous CO_2. This liquid feed not only simplifies the design of the electrolyzer, but also helps to increase CO_2 utilization efficiency and bypasses the need to thermally generate pure CO_2 upstream of the electrolyzer.[26] The CEM also lowers Ohmic resistances relative to an AEM by transporting highly mobile H^+ (ionic mobility 36 × 10^{-8} m^2 s^{-1} V^{-1}) instead of OH^- (ionic mobility 21 × 10^{-8} m^2 s^{-1} V^{-1}; note that CO_3^{2-} is actually the dominant charge carrier in current AEM CO2RR electrolyzers and is characterized by an even lower ionic mobility of 7.5 × 10^{-8} m^2 s^{-1} V^{-1}).[13,15,34] Moreover, CEMs avoid the high water dissociation overpotential associated with BPMs. The transport of H^+ by the CEM into the cathode compartment enables the conversion of bicarbonate into electrochemically active CO_2 at the cathode (eq 4). The oxidation of hydrogen gas instead of water at the anode also serves to lower the applied potential required to drive electrolysis. These collective features of our electrolyzer (denoted "**HOR|CEM|HCO_3^-**" to reflect the configuration) enabled a partial current density for CO of 220 mA cm^{-2} at a cell voltage of 2.3 ± 0.1 V and a CO_2 utilization efficiency of 40 ± 2%. The lowest previously reported voltage for a CO2RR electrolyzer that operates at a partial current density for CO >200 mA cm^{-2} is 2.8 V and 16% CO_2 utilization.[35]

RESULTS AND DISCUSSION

The **HOR|CEM|HCO_3^-** electrolyzer reported here presses the anode and cathode tightly against opposite faces of Nafion, a CEM (Figure 1). Flowplates with serpentine channels were used to deliver humidified H_2 gas and 3 M $KHCO_3$ to the anode and cathode, respectively. The gas diffusion electrode (GDE) in the anode chamber consisted of platinum on carbon black, while a silver-foam electrode was used in the cathode chamber. This electrolyzer was used to perform electrolysis experiments at applied current densities over a 100−1000 mA cm^{-2} range. Product formation rates of CO and H_2 from the

https://doi.org/10.1021/acscentsci.2c00329
ACS Cent. Sci. 2022, 8, 749−755

cathode compartment along with V_{cell} values (the cell voltage measured across the anode and cathode) were recorded over the course of the electrolysis experiments. Measurements of the unreacted H_2 from the anode showed H_2 utilization values of up to 28% (Figure S2). The electrolysis experiments were performed under different pressures using a custom-made pressurized electrolyzer test station (Figure S3).[19]

Electrolysis experiments using this reactor architecture at an applied current density of 100 mA cm^{-2} and ambient conditions yielded a V_{cell} value of 1.7 ± 0.1 V (Figure 2).

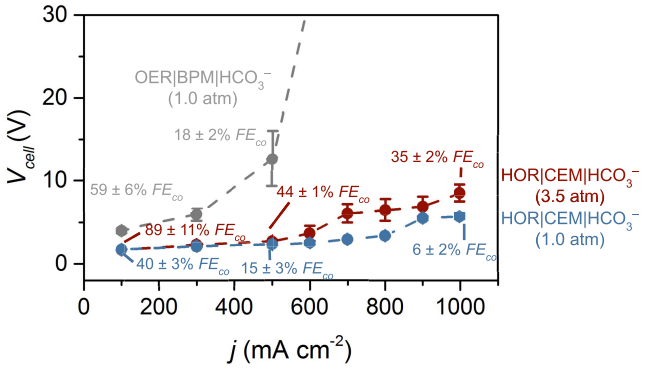

Figure 2. Voltage and current characteristics of an electrolyzer that couples bicarbonate conversion with hydrogen oxidation. V_{cell} values were measured as a function of current density from 100 to 1000 mA cm^{-2} for the **OER|BPM|HCO_3^-** and **HOR|CEM|HCO_3^-** electrolyzers under 1.0 and 3.5 atm of pressure. At 3.5 atm, 50 μm Nafion was used in the **HOR|CEM|HCO_3^-** electrolyzer instead of 25 μm Nafion. Faradaic efficiencies for CO production (FE_{CO}) for each electrolyzer are annotated at discrete points.

This value represents the lowest V_{cell} value ever reported for a liquid-fed CO2RR electrolyzer. When the current density was held at 500 mA cm^{-2}, the V_{cell} value was measured to be 2.3 ± 0.1 V, setting a new benchmark for CO_2 electrolysis.

We plotted V_{cell} values over a range of current densities against those obtained with our previously reported bicarbonate electrolyzer **OER|BPM|HCO_3^-** (Figure 2). The **OER|BPM|HCO_3^-** electrolyzer contains a BPM (instead of Nafion) and mediates the OER at a nickel anode (instead of the HOR at a platinum anode). In order to maintain a current density of 100 mA cm^{-2}, **OER|BPM|HCO_3^-** required a V_{cell} value of 4.0 ± 0.3 V. This value is more than twice as high as that for **HOR|CEM|HCO_3^-**, which performs the HOR at the anode. The V_{cell} value of **OER|BPM|HCO_3^-** spiked to 12.7 ± 3.3 V at 500 mA cm^{-2}, whereas the V_{cell} value of **HOR|CEM|HCO_3^-** was only 2.3 ± 0.1 V at this current density (Figure 2). The low measured voltage of **HOR|CEM|HCO_3^-** relative to **OER|BPM|HCO_3^-** is due not only to the lower thermodynamic voltage limit (achieved by substituting the OER for the HOR), but also the lower overpotentials of the HOR in comparison to the OER and water dissociation reaction (Figure S4).[5,36] The thinner CEM also reduces Ohmic resistances relative to the BPM (the CEM is 25 or 50 μm, whereas the BPM is 195 μm).[37,38] The voltage penalties for water dissociation and the OER render the V_{cell} value for the **OER|BPM|HCO_3^-** electrolyzer impractical.

While the V_{cell} values for **HOR|CEM|HCO_3^-** are state of the art, the measured Faradaic efficiencies for CO production (FE_{CO}) were merely 40 ± 3% at 100 mA cm^{-2} (15 ± 3% at 500 mA cm^{-2}; Figure 2). A supply of H^+ from the membrane to the cathode is required for *in situ* CO_2 (*i*-CO_2) generation (eq 4); however, this H^+ flux can contribute to the parasitic hydrogen evolution reaction (HER). We therefore added a buffer layer between the cathode and membrane to mitigate the HER by managing H^+ transport to the cathode.[39] This buffer layer increased the FE_{CO} value from 40% to 71% at 100 mA cm^{-2} (Figure S5).

We increased the FE_{CO} values even further by pressurizing the bicarbonate feedstock, which increases the CO_2 solubility.[19] The pressurized **HOR|CEM|HCO_3^-** electrolyzer under 3.5 atm of pressure yielded a FE_{CO} value of 89 ± 11% at 100 mA cm^{-2} and 44 ± 1% at 500 mA cm^{-2} (Figure 2). The molar composition of the gaseous cathode outlet stream at 500 mA cm^{-2} was 30% CO_2(g), 22% CO(g), and 48% H_2(g). The **HOR|CEM|HCO_3^-** electrolyzer therefore achieved a j_{CO} value of ∼220 mA cm^{-2}, the highest value reported for CO2RR electrolyzers using a liquid feedstock (Figures S6 and S7). Importantly, the CO_2 utilization value was measured to be 40 ± 2%, which is higher than that for any **OER|AEM|CO_2** electrolyzer which achieves j_{CO} > 200 mA cm^{-2}.[18] The cell voltage was stable for 10 h. The slight decrease in FE_{CO} values could be caused by degradation of the platinum anode catalyst over time (Figure S8).[40]

The **HOR|CEM|HCO_3^-** electrolyzer uses (i) a reactive carbon solution feedstock to bypass CO_2 desorption upstream of the electrolyzer and (ii) the HOR at the anode to eliminate the OER voltage penalty. However, the **OER|AEM|CO_2** electrolyzer achieves a higher FE_{CO} in comparison to the **HOR|CEM|HCO_3^-** electrolyzer, and it does not require H_2 gas. We therefore performed a mass and energy balance to compare these two types of electrolyzer architectures. This analysis encompasses the energy required for the capture, regeneration, and electrolysis of 100 mol of CO_2. Importantly, the analysis accounts for the CO_2 utilization efficiency of each electrolyzer. The Sankey diagram in Figure 3 illustrates how a **HOR|CEM|HCO_3^-** electrolyzer with a CO_2 utilization efficiency of 40% yields CO with a higher energy efficiency (1.4 MJ mol^{-1} CO) in comparison to a **OER|AEM|CO_2** electrolyzer (1.9 MJ mol^{-1} CO) operating at a CO_2 utilization efficiency of 20%.[17] Another advantage of bicarbonate electrolysis is that it does not require the high temperatures and pressures used for thermochemical CO_2 hydrogenation.[41]

While the Sankey diagram shows that the **HOR|CEM|HCO_3^-** consumes less energy than the **OER|AEM|CO_2** electrolyzer, it requires H_2 gas to be fed to the anode. This reaction reduces electricity consumption relative to the OER, but the source and cost of H_2 must be considered. Ideally, H_2 would be produced from a low-carbon source such as biomass gasification or water electrolysis.[44] The cost of generating H_2 by biomass gasification is reported to be as low as $0.9/kg[45,46] (with net negative emissions of 15−22 kg CO_2/kg H_2 when it is coupled to carbon capture and sequestration[47,48]), and the target price for clean H_2 determined by the DOE Energy Earthshots Initiative is $1 per kg of H_2.[49] We therefore used a forward-looking purchase price of $1/kg of H_2 as a basis for comparing the economics of **HOR|CEM|HCO_3^-**, which consumes H_2, to the **OER|BPM|HCO_3^-** and conventional **OER|AEM|CO_2**, which consume water at the anode (Table 1 and Figure S9). We adopted widely used assumptions for future market conditions for this analysis (electricity $0.03/kWh, $50/tonne CO_2, CO sale price of $0.60/kg)[7] and electrolyzer performance specifications (voltages, Faradaic efficiencies, CO_2 utilization efficiencies) for each of the three

https://doi.org/10.1021/acscentsci.2c00329
ACS Cent. Sci. 2022, 8, 749−755

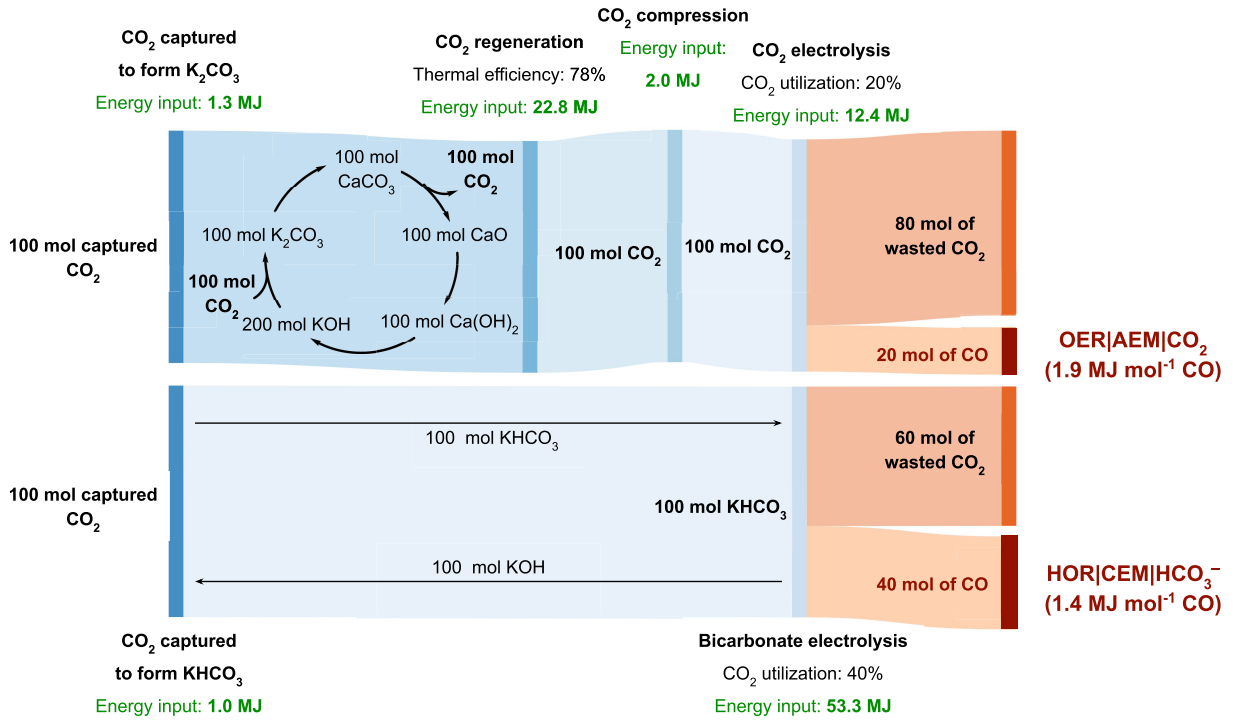

Figure 3. Sankey diagrams illustrating CO_2 mass flows and energy inputs for the capture and conversion of atmospheric CO_2 into CO using an anion exchange membrane (AEM) electrolyzer. The top panel assumes that captured CO_2 is regenerated using a direct air capture process[30,42] and that the electrolyzer is fed with a compressed CO_2 feed (Faradaic efficiency for CO production, FE_{CO} = 90%; V_{cell} = 3.0 V; CO_2 utilization efficiency 20%; J = 500 mA cm^{-2}). The bottom panel relies on the electrolysis of $KHCO_3$ and bypasses the CO_2 regeneration and compression steps (FE_{CO} = 50%; V_{cell} = 2.5 V; CO_2 utilization efficiency 40%; J = 500 mA cm^{-2}). Energy inputs are sourced from refs 30 and 42. The bicarbonate electrolysis pathway analysis accounts for the energy required to generate H_2 from a water electrolyzer (347 kJ mol^{-1} H_2).[43] Details are provided in Table S1.

electrolyzer technologies (Figure S9). We assumed FE_{CO} values of 100% for the **OER|AEM|CO_2** and 80% for the **HOR|CEM|HCO_3^-** and **OER|BPM|HCO_3^-** electrolyzers, assumed a current density of 500 mA cm^{-2}, and expressed the voltages as slightly better than current state of the art metrics for the three electrolyzer technologies (Table 1). To determine the CO_2 capture and separation costs, we used CO_2 utilization efficiencies of 20% for the **OER|AEM|CO_2** and 40% for the **HOR|CEM|HCO_3^-** and **OER|BPM|HCO_3^-** electrolyzers.

The outcome of this technoeconomic analysis is that the **HOR|CEM|HCO_3^-** electrolyzer is the most profitable option of the three electrolyzers (see NPV values in Table 1). The primary drivers for the profitability of a bicarbonate electrolyzer coupled to a H_2 production plant are: (i) the lower electricity costs due to the lower operating voltage; (ii) the lower CO_2 capture and separation costs due to the elimination of CO_2 regeneration; and (iii) the higher CO_2 utilization efficiencies. We note that the recycling of H_2 can further minimize costs. For example, the proof of concept experiments in Figure S10 demonstrate that the amount of virgin H_2 supplied to the system can be reduced by recycling H_2 during the production of formate at the cathode. Formate was targeted for this experiment because CO poisons platinum catalysts used for the HOR and would therefore need to be separated before recycling.[50]

We demonstrate here an electrolyzer that mediates the conversion of reactive carbon solutions enriched with bicarbonate into CO with a partial current density of 220 mA cm^{-2} at merely 2.3 V. This high CO formation rate and low voltage set a benchmark for reactive carbon capture. The CO_2 utilization value of 40% is also state of the art at high current densities (i.e., 500 mA cm^{-2}). By sourcing H^+ from the HOR instead of the OER, the **HOR|CEM|HCO_3^-** electrolyzer requires 2.3 V to drive bicarbonate electrolysis at 500 mA cm^{-2} instead of 12.7 V for **OER|BPM|HCO_3^-**. Moreover, we show that the FE_{CO} value of the electrolyzer can be increased to 89% at 100 mA cm^{-2} and 44% at 500 mA cm^{-2} by pressurizing the electrolyzer to increase CO_2 solubility. With these performance parameters, our technoeconomic analysis (TEA) shows that coupling the HOR with bicarbonate electrolysis can generate CO more profitably than a traditional **OER|AEM|CO_2** electrolyzer. These findings demonstrate a practical method for producing value-added carbon products from reactive carbon capture with low electrical energy input.

METHODS

$KHCO_3$ (99.5%, Alfa Aesar, USA), 50 wt % platinum on Vulcan XC 72 nanopowder (PK catalyst), and ethylenediaminetetraacetic acid (EDTA; 99%, Sigma-Aldrich, USA) were purchased and used as received. Carbon cloth gas diffusion layers (GDLs; Sigracet 39BB), Fumasep FBM bipolar membranes (BPMs), and Nafion PFSA NR-211 and 212 were purchased from Fuel Cell Store (USA). The BPMs were stored in 1 M NaCl, and the Nafion membranes were stored in 1 M KOH prior to use. Silver foams were obtained from Jiangsu Green Materials Hi-Tech. Co. Ltd. (China). Nafion 117 solutions (5 wt %; in a mixture of lower aliphatic alcohols and water) were obtained from Sigma-Aldrich, USA.

https://doi.org/10.1021/acscentsci.2c00329
ACS Cent. Sci. 2022, 8, 749−755

Table 1. Input and Output Parameters from the Technoeconomic Analysis of Three Electrolyzers

	HOR|CEM|HCO_3^-	OER|BPM|HCO_3^-	OER|AEM|CO_2
Input Parameters			
voltage (V)	2	4	3
CO_2 utilization (%)	80	80	40
FE_{CO} (%)	80	80	100
j (mA cm^{-2})		500	
gross cost of CO_2 capture ($/ton)		50	
installed capex cost ($/kW)		450	
electricity ($/kWh)		0.03	
H_2 purchase price ($/kg)	1	N/A	N/A
Output Parameters			
cost of H_2 ($M/yr)	2.61	0.00	0.00
electricity cost ($M/yr)	5.24	10.48	6.29
CO_2 capture cost ($M/yr)	1.06	1.06	2.87
CO_2 separation cost ($M/yr)	0.72	0.72	4.30
maintenance and water cost ($M/yr)	0.25	0.49	0.3
total opex ($M/yr)	**9.88**	**12.75**	**13.75**
total capex: electrolyzer + balance of plant ($M)	**13.8**	**27.6**	**16.56**
Revenue from Sale of CO at $0.60/kg ($M/yr)		21.90	
profit	11.52	8.78	7.82
NPV 20 years[a]	**48.96**	**23.7**	**28.08**

[a]The net present value (NPV) was calculated on the basis of a 20 year plant life, 10% interest rate, 38.9% income tax rate, 2.5% fixed operating cost, and a depreciation schedule based on the modified accelerated cost recovery system that was developed by the Department of Energy for water electrolyzer and hydrogen technologies.

A CH instrument 660D potentiostat (USA) equipped with an Amp booster, and Keithley Precision Measurment DC Supply were used for electrolysis experiments. An Ag/AgCl (3 M NaCl) reference electrode (BASi) was used for cathode potential measurements. A gas chromatography instrument (GC; PerkinElmer, Clarus 580), equipped with a packed MolSieve 5 Å column and a packed HayeSepD column, was used to detect CO and H_2 using a flame ionization detector (FID) and a thermal conductivity detector (TCD), respectively. The concentrations of the products CO and H_2 (ppm) in the headspace of the catholyte reservoir were quantified by calibrating the signal area for CO and H_2 to known concentrations of the two gases.

Electrode Preparation. The silver foam was cut into the desired dimensions (2 × 2 cm) with a blade and washed with acetone and water. The silver foam was treated with dilute nitric acid solution (30% v/v HNO_3) in a 50 mL beaker for 10 s to remove the oxide layer and increase its electrochemical surface area. The etched silver foam was then washed thoroughly with deionized (DI) water and 3 M $KHCO_3$ prior to use.

To fabricate the Pt/C gas diffusion electrode (GDE), 8 mg of Pt/C was added to a 2.5 mL mixture of water and isopropanol (IPA) solution (V_{H2O}:V_{IPA} = 4:1) with 20 wt % Nafion solution (5 wt %). The ink was sonicated in a bath sonicator for 15 min and then drop-casted onto a GDL. The fabricated GDEs were then stored in a fume hood to dry overnight.

Electrolysis. A peristaltic pump was used to deliver 1.0 M KOH to the anode of the control system at a constant flow rate of 40 mL min^{-1}. High-purity H_2 (10−200 sccm, 99.999%) was humidified in a bubbler held at a constant temperature of 60 °C prior to being fed to the anode of **HOR|CEM|HCO_3^-** (Figure S5). Two 127 μm polytetrafluoroethylene (PTFE) gaskets were placed separately between the anode and anodic flowplate and the cathode and cathodic flowplate to prevent leakage for all of the electrolyzers. The catholyte (3.0 M $KHCO_3$) was delivered at a constant flow rate of 100 mL min^{-1} for all electrolyzers. Gaseous products (e.g., H_2 and CO) in the headspace of the cathode electrolyte reservoir were delivered to an in-line gas chromatograph (GC) by a constant rate of N_2 flow at 175 sccm for quantification at 350 s. The actual flow rate of the gas mixture was measured by a flow meter positioned immediately downstream of the GC. Liquid products collected from the catholyte after 1200 s of electrolysis were quantified by ^{1}H NMR spectroscopy using potassium hydrogen phthalate as the internal standard with a calibration curve.

Safety Statement. No unexpected or unusually high safety hazards were encountered.

■ ASSOCIATED CONTENT

Supporting Information

The Supporting Information is available free of charge at https://pubs.acs.org/doi/10.1021/acscentsci.2c00329.

Faradaic efficiency calculation, liquid product detection, CO_2 utilization calculation, pressurized electrolyzer test station, technoeconomic analysis, energy consumption analysis (Sankey diagram), diagram of the experimental setup, the effect of the H_2 flow rate on the cell voltage and FE_{CO}, membrane thickness effect, V_{cell}−j_{CO} relationship, stability test, and H_2 recycling data (PDF)

■ AUTHOR INFORMATION

Corresponding Author

Curtis P. Berlinguette − *Department of Chemistry, The University of British Columbia, Vancouver, British Columbia V6T 1Z1, Canada; Department of Chemical and Biological Engineering, The University of British Columbia, Vancouver, British Columbia V6T 1Z3, Canada; Stewart Blusson Quantum Matter Institute, The University of British Columbia, Vancouver, British Columbia V6T 1Z4, Canada; Canadian Institute for Advanced Research (CIFAR), Toronto, Ontario M5G 1M1, Canada;* orcid.org/0000-0001-6875-849X; Email: cberling@chem.ubc.ca

Authors

Zishuai Zhang − *Department of Chemistry, The University of British Columbia, Vancouver, British Columbia V6T 1Z1, Canada*

Eric W. Lees − *Department of Chemical and Biological Engineering, The University of British Columbia, Vancouver, British Columbia V6T 1Z3, Canada*

Shaoxuan Ren − *Department of Chemistry, The University of British Columbia, Vancouver, British Columbia V6T 1Z1, Canada*

Benjamin A. W. Mowbray − *Department of Chemistry, The University of British Columbia, Vancouver, British Columbia V6T 1Z1, Canada;* orcid.org/0000-0001-9452-2931

https://doi.org/10.1021/acscentsci.2c00329
ACS Cent. Sci. 2022, 8, 749−755

Aoxue Huang − *Department of Chemistry, The University of British Columbia, Vancouver, British Columbia V6T 1Z1, Canada;* orcid.org/0000-0003-2507-0198

Complete contact information is available at: https://pubs.acs.org/10.1021/acscentsci.2c00329

Author Contributions

⊥Z.Z. and E.W.L. contributed equally to this work.

Author Contributions

C.P.B. supervised the project. Z.Z. and C.P.B. conceived the study, and Z.Z. performed the experiments. E.W.L. designed the pressurized system, performed the technoeconomic analysis, and determined the mass and energy balances. S.R. performed experiments and an analysis and aided in technical editing. B.A.W.M. performed an analysis and aided in writing and technical editing. A.H. contributed to an analysis of experimental data. C.P.B., Z.Z., and E.W.L. wrote the first draft of the manuscript. All authors contributed to the writing of the final manuscript.

Notes

The authors declare the following competing financial interest(s): The authors C.P.B. and Z.Z. have filed a patent related to this work (No. PCT/CA2022/050094; US patent application No. 63/140.167).

■ ACKNOWLEDGMENTS

The authors are grateful to Dr. Roxanna Delima and Dr. Yong Wook Kim for their valuable suggestions and discussions. The authors are grateful to Natural Resources Canada (EIP2-MAT-001), the Canadian Natural Science and Engineering Research Council (CRDPJ 536621-18), the Canadian Foundation for Innovation (229288), the Canadian Institute for Advanced Research (BSE-BERL-162173), TOTAL American Services, Inc. (an affiliate of TotalEnergies SE, France), and the Canada Research Chairs for financial support. This research was undertaken thanks in part to funding from the Canada First Research Excellence Fund, Quantum Materials and Future Technologies Program. Supplementary data sets generated in the current study are available from the corresponding author upon reasonable request.

■ REFERENCES

(1) Weekes, D. M.; Salvatore, D. A.; Reyes, A.; Huang, A.; Berlinguette, C. P. Electrolytic CO_2 Reduction in a Flow Cell. *Acc. Chem. Res.* **2018**, *51* (4), 910−918.

(2) Whipple, D. T.; Kenis, P. J. A. Prospects of CO2 Utilization via Direct Heterogeneous Electrochemical Reduction. *J. Phys. Chem. Lett.* **2010**, *1* (24), 3451−3458.

(3) Hori, Y. Electrochemical CO2 Reduction on Metal Electrodes. In *Modern Aspects of Electrochemistry*; Vayenas, C. G., White, R. E., Gamboa-Aldeco, M. E., Eds.; Springer New York: 2008; pp 89−189.

(4) Nitopi, S.; Bertheussen, E.; Scott, S. B.; Liu, X.; Engstfeld, A. K.; Horch, S.; Seger, B.; Stephens, I. E. L.; Chan, K.; Hahn, C.; Nørskov, J. K.; Jaramillo, T. F.; Chorkendorff, I. Progress and Perspectives of Electrochemical CO2 Reduction on Copper in Aqueous Electrolyte. *Chem. Rev.* **2019**, *119* (12), 7610−7672.

(5) Salvatore, D.; Berlinguette, C. P. Voltage Matters When Reducing CO_2 in an Electrochemical Flow Cell. *ACS Energy Letters* **2020**, *5*, 215.

(6) Spurgeon, J. M.; Kumar, B. A Comparative Technoeconomic Analysis of Pathways for Commercial Electrochemical CO_2 Reduction to Liquid Products. *Energy Environ. Sci.* **2018**, *11* (6), 1536−1551.

(7) Jouny, M.; Luc, W.; Jiao, F. General Techno-Economic Analysis of CO_2 Electrolysis Systems. *Ind. Eng. Chem. Res.* **2018**, *57* (6), 2165−2177.

(8) De Luna, P.; Hahn, C.; Higgins, D.; Jaffer, S. A.; Jaramillo, T. F.; Sargent, E. H. What Would It Take for Renewably Powered Electrosynthesis to Displace Petrochemical Processes? *Science* **2019**, *364* (6438), eaav3506.

(9) Endrődi, B.; Kecsenovity, E.; Samu, A.; Halmágyi, T.; Rojas-Carbonell, S.; Wang, L.; Yan, Y.; Janáky, C. High Carbonate Ion Conductance of a Robust PiperION Membrane Allows Industrial Current Density and Conversion in a Zero-Gap Carbon Dioxide Electrolyzer Cell. *Energy Environ. Sci.* **2020**, *13* (11), 4098−4105.

(10) Yin, Z.; Peng, H.; Wei, X.; Zhou, H.; Gong, J.; Huai, M.; Xiao, L.; Wang, G.; Lu, J.; Zhuang, L. An Alkaline Polymer Electrolyte CO_2 Electrolyzer Operated with Pure Water. *Energy Environ. Sci.* **2019**, *12*, 2455−2462. 2019

(11) Verma, S.; Lu, S.; Kenis, P. J. A. Co-Electrolysis of CO_2 and Glycerol as a Pathway to Carbon Chemicals with Improved Technoeconomics due to Low Electricity Consumption. *Nature Energy* **2019**, *4* (6), 466.

(12) Endrődi, B.; Samu, A.; Kecsenovity, E.; Halmágyi, T.; Sebők, D.; Janáky, C. Operando Cathode Activation with Alkali Metal Cations for High Current Density Operation of Water-Fed Zero-Gap Carbon Dioxide Electrolyzers. *Nat. Energy* **2021**, *6* (4), 439−448.

(13) Lees, E. W.; Mowbray, B. A. W.; Parlane, F. G.; Berlinguette, C. P. Gas Diffusion Electrodes and Membranes for CO_2 Reduction Electrolyzers. *Nature Reviews Materials* **2022**, *7*, 55−64.

(14) Rabinowitz, J. A.; Kanan, M. W. The Future of Low-Temperature Carbon Dioxide Electrolysis Depends on Solving One Basic Problem. *Nat. Commun.* **2020**, *11* (1), 5231.

(15) Larrazábal, G. O.; Strøm-Hansen, P.; Heli, J. P.; Zeiter, K.; Therkildsen, K. T.; Chorkendorff, I.; Seger, B. Analysis of Mass Flows and Membrane Cross-over in CO_2 Reduction at High Current Densities in an MEA-Type Electrolyzer. *ACS Appl. Mater. Interfaces* **2019**, *11* (44), 41281−41288.

(16) Ma, M.; Clark, E. L.; Therkildsen, K. T.; Dalsgaard, S.; Chorkendorff, I.; Seger, B. Insights into the Carbon Balance for CO_2 Electroreduction on Cu Using Gas Diffusion Electrode Reactor Designs. *Energy Environ. Sci.* **2020**, *13* (3), 977−985.

(17) Jeng, E.; Jiao, F. Investigation of CO_2 Single-Pass Conversion in a Flow Electrolyzer. *Reaction Chemistry & Engineering* **2020**, *5* (9), 1768−1775.

(18) Bhargava, S. S.; Proietto, F.; Azmoodeh, D.; Cofell, E. R.; Henckel, D. A.; Verma, S.; Brooks, C. J.; Gewirth, A. A.; Kenis, P. System Design Rules for Intensifying the Electrochemical Reduction of CO_2 to CO on Ag Nanoparticles. *ChemElectroChem.* **2020**, *7* (9), 2001−2011.

(19) Zhang, Z.; Lees, E. W.; Habibzadeh, F.; Salvatore, D. A.; Ren, S.; Simpson, G. L.; Wheeler, D. G.; Liu, A.; Berlinguette, C. P. Porous Metal Electrodes Enable Efficient Electrolysis of Carbon Capture Solutions. *Energy Environ. Sci.* **2022**, *15*, 705−713.

(20) Lees, E. W.; Goldman, M.; Fink, A. G.; Dvorak, D. J.; Salvatore, D. A.; Zhang, Z.; Loo, N. W. X.; Berlinguette, C. P. Electrodes Designed for Converting Bicarbonate into CO. *ACS Energy Letters* **2020**, *5*, 2165−2173.

(21) Yang, K.; Li, M.; Subramanian, S.; Blommaert, M. A.; Smith, W. A.; Burdyny, T. Cation-Driven Increases of CO2 Utilization in a Bipolar Membrane Electrode Assembly for CO_2 Electrolysis. *ACS Energy Lett.* **2021**, *6* (12), 4291−4298.

(22) O'Brien, C. P.; Miao, R. K.; Liu, S.; Xu, Y.; Lee, G.; Robb, A.; Huang, J. E.; Xie, K.; Bertens, K.; Gabardo, C. M.; Edwards, J. P.; Dinh, C.-T.; Sargent, E. H.; Sinton, D. Single Pass CO_2 Conversion Exceeding 85% in the Electrosynthesis of Multicarbon Products via Local CO_2 Regeneration. *ACS Energy Lett.* **2021**, *6* (8), 2952−2959.

(23) Lees, E. W.; Bui, J. C.; Song, D.; Weber, A. Z.; Berlinguette, C. P. Continuum Model to Define the Chemistry and Mass Transfer in a Bicarbonate Electrolyzer. *ACS Energy Lett.* **2022**, *7*, 834−842.

(24) Luo, J.; Vermaas, D. A.; Bi, D.; Hagfeldt, A.; Smith, W. A.; Grätzel, M. Bipolar Membrane-Assisted Solar Water Splitting in Optimal pH. *Adv. Energy Mater.* **2016**, *6* (13), 1600100.
(25) Oener, S. Z.; Foster, M. J.; Boettcher, S. W. Accelerating Water Dissociation in Bipolar Membranes and for Electrocatalysis. *Science* **2020**, *369* (6507), 1099−1103.
(26) Li, T.; Lees, E. W.; Goldman, M.; Salvatore, D. A.; Weekes, D. M.; Berlinguette, C. P. Electrolytic Conversion of Bicarbonate into CO in a Flow. *Cell. Joule* **2019**, *3* (6), 1487−1497.
(27) Li, T.; Lees, E. W.; Zhang, Z.; Berlinguette, C. P. Conversion of Bicarbonate to Formate in an Electrochemical Flow Reactor. *ACS Energy Lett.* **2020**, *5*, 2624−2630.
(28) Li, Y. C.; Zhou, D.; Yan, Z.; Gonçalves, R. H.; Salvatore, D. A.; Berlinguette, C. P.; Mallouk, T. E. Electrolysis of CO2 to Syngas in Bipolar Membrane-Based Electrochemical Cells. *ACS Energy Lett.* **2016**, *1* (6), 1149−1153.
(29) Diaz, L. A.; Gao, N.; Adhikari, B.; Lister, T. E.; Dufek, E. J.; Wilson, A. D. Electrochemical Production of Syngas from CO2 Captured in Switchable Polarity Solvents. *Green Chemistry.* **2018**, *20*, 620−626.
(30) Keith, D. W.; Holmes, G.; St. Angelo, D.; Heidel, K. A Process for Capturing CO_2 from the Atmosphere. *Joule* **2018**, *2* (8), 1573−1594.
(31) Smith, W. A.; Burdyny, T.; Vermaas, D. A.; Geerlings, H. Pathways to Industrial-Scale Fuel Out of Thin Air from CO2 Electrolysis. *Joule* **2019**, *3* (8), 1822−1834.
(32) Luyben, W. L. Capital Cost of Compressors for Conceptual Design. *Chemical Engineering and Processing - Process Intensification* **2018**, *126*, 206−209.
(33) Alerte, T.; Edwards, J. P.; Gabardo, C. M.; O'Brien, C. P.; Gaona, A.; Wicks, J.; Obradović, A.; Sarkar, A.; Jaffer, S. A.; MacLean, H. L.; Sinton, D.; Sargent, E. H. Downstream of the CO_2 Electrolyzer: Assessing the Energy Intensity of Product Separation. *ACS Energy Lett.* **2021**, *6*, 4405−4412.
(34) Weng, L.-C.; Bell, A. T.; Weber, A. Z. Towards Membrane-Electrode Assembly Systems for CO_2 Reduction: A Modeling Study. *Energy Environ. Sci.* **2019**, *12* (6), 1950−1968.
(35) Garcia de Arquer, F. P.; Dinh, C.-T.; Ozden, A.; Wicks, J.; McCallum, C.; Kirmani, A. R.; Nam, D.-H.; Gabardo, C.; Seifitokaldani, A.; Wang, X.; Li, Y. C.; Li, F.; Edwards, J.; Richter, L. J.; Thorpe, S. J.; Sinton, D.; Sargent, E. H. CO2 Electrolysis to Multicarbon Products at Activities Greater than 1 A cm^{-2}. *Science* **2020**, *367* (6478), 661−666.
(36) Vermaas, D. A.; Wiegman, S.; Nagaki, T.; Smith, W. A. Ion Transport Mechanisms in Bipolar Membranes for (photo) Electrochemical Water Splitting. *Sustainable Energy & Fuels* **2018**, *2* (9), 2006−2015.
(37) Blommaert, M. A.; Vermaas, D. A.; Izelaar, B.; in 't Veen, B.; Smith, W. A. Electrochemical Impedance Spectroscopy as a Performance Indicator of Water Dissociation in Bipolar Membranes. *J. Mater. Chem. A Mater. Energy Sustain.* **2019**, 7 (32), 19060−19069.
(38) Santana, J.; Espinoza-Andaluz, M.; Li, T.; Andersson, M. A Detailed Analysis of Internal Resistance of a PEFC Comparing High and Low Humidification of the Reactant Gases. *Frontiers in Energy Research* **2020**, *8*, 217.
(39) Salvatore, D. A.; Weekes, D. M.; He, J.; Dettelbach, K. E.; Li, Y. C.; Mallouk, T. E.; Berlinguette, C. P. Electrolysis of Gaseous CO_2 to CO in a Flow Cell with a Bipolar Membrane. *ACS Energy Lett.* **2018**, *3* (1), 149−154.
(40) Albarbar, A.; Alrweq, M. *Proton Exchange Membrane Fuel Cells: Design, Modelling and Performance Assessment Techniques*; Springer: 2017.
(41) Roy, S.; Cherevotan, A.; Peter, S. C. Thermochemical CO2 Hydrogenation to Single Carbon Products: Scientific and Technological Challenges. *ACS Energy Lett.* **2018**, *3* (8), 1938−1966.
(42) Welch, A. J.; Dunn, E.; DuChene, J. S.; Atwater, H. A. Bicarbonate or Carbonate Processes for Coupling Carbon Dioxide Capture and Electrochemical Conversion. *ACS Energy Letters* **2020**, *5* (3), 940−945.
(43) Kauw, M.; Benders, R. M. J.; Visser, C. Green Methanol from Hydrogen and Carbon Dioxide Using Geothermal Energy And/or Hydropower in Iceland or Excess Renewable Electricity in Germany. *Energy* **2015**, *90*, 208−217.
(44) Li, W.; Feaster, J. T.; Akhade, S. A.; Davis, J. T.; Wong, A. A.; Beck, V. A.; Varley, J. B.; Hawks, S. A.; Stadermann, M.; Hahn, C.; Aines, R. D.; Duoss, E. B.; Baker, S. E. Comparative Techno-Economic and Life Cycle Analysis of Water Oxidation and Hydrogen Oxidation at the Anode in a CO_2 Electrolysis to Ethylene System. *ACS Sustainable Chem. Eng.* **2021**, *9* (44), 14678−14689.
(45) Kayfeci, M.; Keçebaş, A.; Bayat, M. Hydrogen Production. In *Solar Hydrogen Production*; Calise, F., D'Accadia, M. D., Santarelli, M., Lanzini, A., Ferrero, D., Eds.; Academic Press: 2019; Chapter 3, pp 45−83.
(46) Baker, S.; Stolaroff, J.; Peridas, G.; Pang, S.; Goldstein, H.; Lucci, F.; Li, W.; Slessarev, E.; Pett-Ridge, J.; Ryerson, F.; Wagoner, J.; Kirkendall, W.; Aines, R.; Sanchez, D.; Cabiyo, B.; Baker, J.; McCoy, S.; Uden, S.; Runnebaum, R.; Wilcox, J.; Psarras, P.; Pilorge, H.; McQueen, N.; Maynard, D.; McCormick, C. *Getting to Neutral: Options for Negative Carbon Emissions in California*; LLNL-TR-796100; Lawrence Livermore National Laboratory (LLNL), 2019. DOI: 10.2172/1597217.
(47) Parkinson, B.; Balcombe, P.; Speirs, J. F.; Hawkes, A. D.; Hellgardt, K. Levelized Cost of CO_2 Mitigation from Hydrogen Production Routes. *Energy Environ. Sci.* **2019**, *12* (1), 19−40.
(48) Salkuyeh, Y. K.; Saville, B. A.; MacLean, H. L. Techno-Economic Analysis and Life Cycle Assessment of Hydrogen Production from Different Biomass Gasification Processes. *Int. J. Hydrogen Energy* **2018**, *43* (20), 9514−9528.
(49) Energy Earthshots Initiative: https://www.energy.gov/policy/energy-earthshots-initiative (accessed 2021-08-25).
(50) Lee, M. J.; Kang, J. S.; Kang, Y. S.; Chung, D. Y.; Shin, H.; Ahn, C.-Y.; Park, S.; Kim, M.-J.; Kim, S.; Lee, K.-S.; Sung, Y.-E. Understanding the Bifunctional Effect for Removal of CO Poisoning: Blend of a Platinum Nanocatalyst and Hydrous Ruthenium Oxide as a Model System. *ACS Catal.* **2016**, *6* (4), 2398−2407.

https://doi.org/10.1021/acscentsci.2c00329
ACS Cent. Sci. 2022, 8, 749−755